# Thermosensitive Unimolecular Micelles Surface-Decorated with Gold Nanoparticles of Tunable Spatial Distribution

Hangxun Xu, Jian Xu, Xiaoze Jiang, Zhiyuan Zhu, Jingyi Rao, Jun Yin, Tao Wu, Hewen Liu, and Shiyong Liu*

*Department of Polymer Science and Engineering, Hefei National Laboratory for Physical Sciences at the Microscale, University of Science and Technology of China, Hefei, Anhui 230026, China*

*Received January 10, 2007. Revised Manuscript Received March 16, 2007*

Gold nanoparticles were covalently conjugated onto the surface of thiol-functionalized thermosensitive unimolecular micelles to fabricate novel satellite-like nanostructures. The resultant nanostructures consist of gold nanoparticles distributed across the surface of isolated unimolecular micelles. Because of the covalent linkage between surface thiol groups and gold nanoparticles, this novel type of hybrid nanostructure was highly stable. Most importantly, the unimolecular micelle templates were thermosensitive and can reversibly swell and shrink in response to external temperatures. This made it possible to finely tune the spatial distances between gold nanoparticles attached at the micelle surface. Therefore, this approach can be extended toward the fabrication of novel nanomaterials with sophisticated structures and tunable multifunctionalities.

## Introduction

Increasing attention has been paid to explore suitable techniques to assemble gold nanoparticles into well-defined nanostructures with controllable dimensions and spatial properties.[1−3] The template-assembling technique has been frequently employed to fabricate one-, two-, and three-dimensional (3D) nanostructured materials, utilizing various interactions, such as covalent, electrostatic, hydrogen bonding, and van der Waals forces.[4−8] For example, 3D nanostructures based on complementary interparticle interactions involving hydrogen-bonding moieties,[9] DNA duplex formation,[10] antigen−antibody,[11] and streptavidin−biotin recognition[12] have been reported.

Controlling the interparticle distances is also truly relevant to the electronic and magnetic properties of nanoparticles,[13] which can be realized by manipulation of the protecting monolayers of self-assembling nanoparticles,[14,15] or usage of separate entities such as polymer scaffolds.[16,17] Noncovalent interactions between nanoparticles and patterned polymer surface can also be utilized to fabricate 2D arrays of nanoparticles.[16,17]

Compared to the noncovalent approaches usually employed for template-assembling, the covalent approach provides to be a quite straightforward technique for assembled nanoparticles with enhanced stability, which are thus suitable for a wider range of applications.[18−21] Huo et al.[19] conjugated mono-carboxyl-functionalized gold nanoparticles onto poly(amidoamine) dendrimers; the interparticle distance can be tuned by the dendrimer generation. Using polylysine as templates, they also obtained a novel type of "nanonecklace" of gold nanoparticles.[18] Park et al.[21] covalently conjugated gold nanoparticles to the thiolated hyaluronic acid polymer chains, and the resultant one-dimensional array of nanoparticles can be employed to directly visualize the chain conformations.

Self-assembled nanostructures of amphiphilic block copolymers in solution can also serve as excellent scaffolds for assembling gold nanoparticles and tuning the interparticle distances. Park et al.[20] covalently attached gold nanoparticles onto surface-thiolated Pluronic micelles to prepare stable shell cross-linked micelles. However, it is well-known that the microstructure of block copolymer micelles is not static and there exists dynamic exchange between micelles and unimers, i.e., they tend to be disintegrated upon alteration

* To whom correspondence should be addressed. E-mail: sliu@ustc.edu.cn.

(1) Alivisatos, A. P. *Science* **1996**, *271*, 933−937.
(2) Daniel, M. C.; Astruc, D. *Chem. Rev.* **2004**, *104*, 293−346.
(3) Shenhar, R.; Rotello, V. M. *Acc. Chem. Res.* **2003**, *36*, 549−561.
(4) Xu, L.; Guo, Y.; Xie, R. G.; Zhuang, J. Q.; Yang, W. S.; Li, T. J. *Nanotechnology* **2002**, *13*, 725−728.
(5) Eustis, S.; El-Sayed, M. A. *Chem. Soc. Rev.* **2006**, *35*, 209−217.
(6) Storhoff, J. J.; Mirkin, C. A. *Chem. Rev.* **1999**, *99*, 1849−1862.
(7) Taton, T. A.; Mirkin, C. A.; Letsinger, R. L. *Science* **2000**, *289*, 1757−1760.
(8) Hicks, J. F.; Zamborini, F. P.; Osisek, A.; Murray, R. W. *J. Am. Chem. Soc.* **2001**, *123*, 7048−7053.
(9) Fullam, S.; Rensmo, H.; Rao, S. N.; Fitzmaurice, D. *Chem. Mater.* **2002**, *14*, 3643−3650.
(10) Mirkin, C. A. *Inorg. Chem.* **2000**, *39*, 2258−2272.
(11) Shenton, W.; Davis, S. A.; Mann, S. *Adv. Mater.* **1999**, *11*, 449-+.
(12) Connolly, S.; Fitzmaurice, D. *Adv. Mater.* **1999**, *11*, 1202−1205.
(13) Shenhar, R.; Norsten, T. B.; Rotello, V. M. *Adv. Mater.* **2005**, *17*, 657−669.
(14) Norsten, T. B.; Frankamp, B. L.; Rotello, V. M. *Nano Lett.* **2002**, *2*, 1345.
(15) Ohno, K.; Koh, K.; Tsujii, Y.; Fukuda, T. *Macromolecules* **2002**, *35*, 8989.
(16) Bockstaller, M. R.; Lapetnikov, Y.; Margel, S.; Thomas, E. L. *J. Am. Ceram. Soc.* **2003**, *125*, 5276.
(17) Zehner, R. W.; Lopes, W. A.; Morkved, T. L.; Jaeger, H.; Sita, L. R. *Langmuir* **1998**, *14*, 241.
(18) Dai, Q.; Worden, J. G.; Trullinger, J.; Huo, Q. *J. Am. Chem. Soc.* **2005**, *127*, 8008−8009.
(19) Worden, J. G.; Dai, Q.; Huo, Q. *Chem. Commun.* **2006**, 1536−1538.
(20) Bae, K. H.; Choi, S. H.; Park, S. Y.; Lee, Y.; Park, T. G. *Langmuir* **2006**, *22*, 6380−6384.
(21) Lee, H.; Choi, S. H.; Park, T. G. *Macromolecules* **2006**, *39*, 23−25.

10.1021/cm070088g CCC: $37.00 
Published on Web 04/14/2007

**Scheme 1. (a) Hybrid Unimolecular Micelles Exhibiting Thermo-Tunable Spatial Distance between Au Nanoparticles Attached at the Micelle Surface and (b) Schematic Illustration of the Two-Step Preparation of Hybrid Unimolecular Micelles Surface Decorated with Au Nanoparticles**

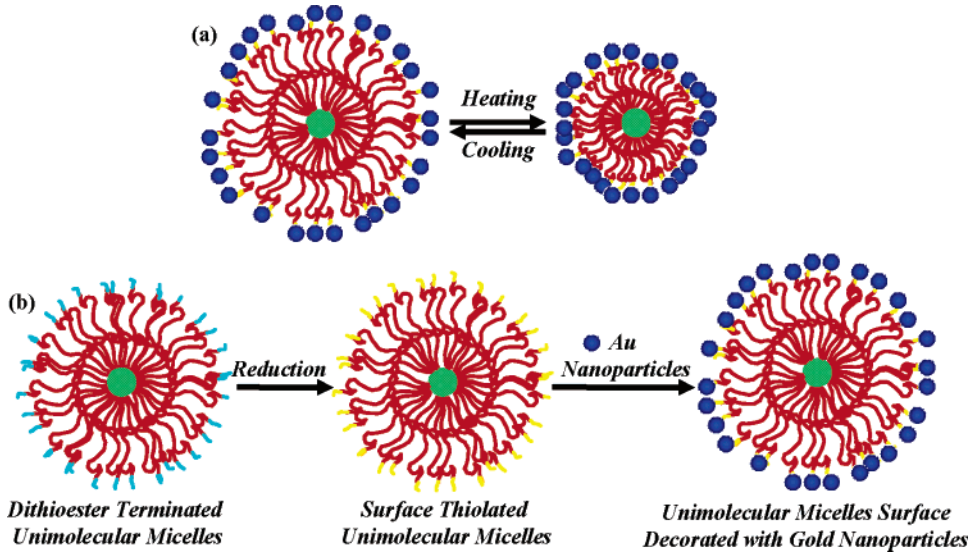


of external conditions such as concentration, temperature, pH, and ionic strengths, etc.[22−25] This disadvantage poses severe limitations to their applications as nanoparticle self-assembling templates. Chemical cross-linking of the micellar core or shell can lead to micelles with permanent stability.[26−35] When hydrophilic polymer chains are tethered to a hydrophobic multifunctional core, such as dendritic macromolecules and star block copolymers, they can be considered as unimolecular micelles because of their structural resemblance to amphiphilic block copolymer micelles.[36−47] Moreover, polymeric unimolecular micelles generally possess well-defined chemical structures with predetermined core size, controllable length, and density of grafted chains, thus they can serve as excellent templates for nanoparticle assembling.[48]

In this paper, we covalently conjugate gold nanoparticles onto the surface of thiol-functionalized thermosensitive unimolecular micelles to fabricate novel satellite-like[49] nanostructures. The resultant nanostructures consist of gold nanoparticles distributed across the surface of isolated unimolecular micelles. Because of the covalent linkage between surface thiol groups and gold nanoparticles, this novel type of hybrid nanostructure is highly stable. Another novelty of our strategy is that the unimolecular micelle templates are thermosensitive and can reversibly swell and shrink in response to external temperatures. This made it possible to finely tune the spatial distances between gold nanoparticles attached at the micelle surface. Scheme 1 illustrates the synthetic scheme of the hybrid satellite-like nanostructures with thermo-tunable spatial distance between Au nanoparticles.

## Experimental Section

**Materials.** Hyperbranched polyester Boltorn H40 was obtained from Perstorp Polyols AB. It was further fractionated with a typical 20% yield using a procedure reported by Tsukruk et al.[50−52] Boltorn

(22) Hamley, I. W. *The Physics of Block Copolymers*; Oxford University Press: Oxford, UK, 1998.
(23) Liu, S. Y.; Billingham, N. C.; Armes, S. P. *Angew. Chem., Int. Ed.* **2001**, *40*, 2328−2331.
(24) Zhang, W. Q.; Shi, L. Q.; Wu, K.; An, Y. G. *Macromolecules* **2005**, *38*, 5743−5747.
(25) Zhang, W. Q.; Shi, L. Q.; An, Y. L.; Gao, L. C.; Wu, K.; Ma, R. J. *Macromolecules* **2004**, *37*, 2551−2555.
(26) Huang, H. Y.; Kowalewski, T.; Remsen, E. E.; Gertzmann, R.; Wooley, K. L. *J. Am. Chem. Soc.* **1997**, *119*, 11653−11659.
(27) Ma, Q. G.; Remsen, E. E.; Kowalewski, T.; Schaefer, J.; Wooley, K. L. *Nano Lett.* **2001**, *1*, 651−655.
(28) Murthy, K. S.; Ma, Q. G.; Remsen, E. E.; Kowalewski, T.; Wooley, K. L. *J. Mater. Chem.* **2003**, *13*, 2785−2795.
(29) Butun, V.; Billingham, N. C.; Armes, S. P. *J. Am. Chem. Soc.* **1998**, *120*, 12135−12136.
(30) Liu, S. Y.; Weaver, J. V. M.; Tang, Y. Q.; Billingham, N. C.; Armes, S. P.; Tribe, K. *Macromolecules* **2002**, *35*, 6121−6131.
(31) Tao, J.; Liu, G. J.; Ding, J. F.; Yang, M. L. *Macromolecules* **1997**, *30*, 4084−4089.
(32) Liu, S. Y.; Weaver, J. V. M.; Save, M.; Armes, S. P. *Langmuir* **2002**, *18*, 8350−8357.
(33) Liu, S. Y.; Armes, S. P. *J. Am. Chem. Soc.* **2001**, *123*, 9910−9911.
(34) Hui, T. R.; Chen, D. Y.; Jiang, M. *Macromolecules* **2005**, *38*, 5834−5837.
(35) Chen, D. Y.; Peng, H. S.; Jiang, M. *Macromolecules* **2003**, *36*, 2576−2578.
(36) Liu, M.; Kono, K.; Frechet, J. M. J. *J. Controlled Release* **2000**, *65*, 121−131.
(37) Aathimanikandan, S. V.; Savariar, E. N.; Thayumanavan, S. *J. Am. Chem. Soc.* **2005**, *127*, 14922−14929.
(38) Zhao, Y. L.; Chen, Y. M.; Chen, C. F.; Xi, F. *Polymer* **2005**, *46*, 5808−5819.
(39) Gillies, E. R.; Frechet, J. M. J. *Drug Discovery Today* **2005**, *10*, 35−43.
(40) Haag, R. *Angew. Chem., Int. Ed.* **2004**, *43*, 278−282.
(41) Thayumanavan, S.; Bharathi, P.; Sivanandan, K.; Vutukuri, D. R. *C. R. Chim.* **2003**, *6*, 767−778.
(42) Jones, M. C.; Ranger, M.; Leroux, J. C. *Bioconjugate Chem.* **2003**, *14*, 774−781.
(43) Yusa, S.; Sakakibara, A.; Yamamoto, T.; Morishima, Y. *Macromolecules* **2002**, *35*, 10182−10188.
(44) Heise, A.; Hedrick, J. L.; Frank, C. W.; Miller, R. D. *J. Am. Chem. Soc.* **1999**, *121*, 8647−8648.
(45) Hawker, C. J.; Wooley, K. L.; Frechet, J. M. J. *J. Chem. Soc., Perkin Trans. 1* **1993**, 1287−1297.
(46) You, Y. Z.; Hong, C. Y.; Pan, C. Y.; Wang, P. H. *Adv. Mater.* **2004**, *16*, 1953-+.
(47) Zheng, Q.; Pan, C. Y. *Macromolecules* **2005**, *38*, 6841−6848.
(48) Xu, H. X.; Xu, J.; Zhu, Z. Y.; Liu, H.; Liu, S. Y. *Macromolecules* **2006**, *39*, 8451−8455.
(49) Yi, D. K.; Lee, S. S.; Ying, J. Y. *Chem. Mater.* **2006**, *18*, 2459−2461.

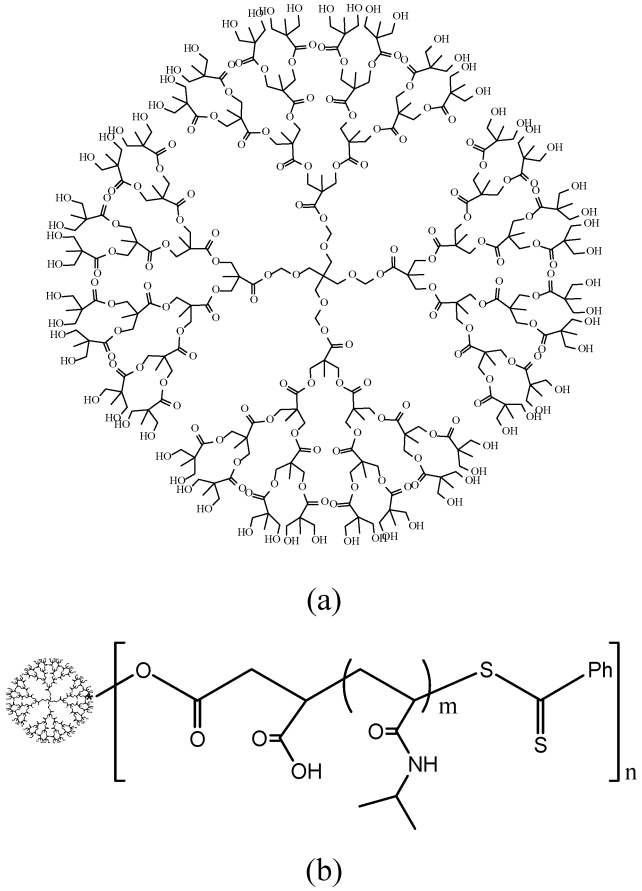


**Figure 1.** (a) Idealized molecular structure of H40; (b) the chemical structure of H40-PNIPAM.

H40 as an ideal dendrimer would theoretically have 64 primary hydroxyl groups and a molar mass of 7316 g mo−1; its ideal chemical structure is shown in Figure 1. SEC analysis of fractionated Boltorn H40 indicated an $M_n$ of 6500 g mol$^{-1}$ and a polydispersity of 1.40.[53] We denote the fractionated hyperbranched polyester as H40 here. According to Tsukruk et al.,[51] the degree of branching of *H40* was 0.4 and the average number of monomeric units (the degree of polymerization) was ca. 60. *N*-Isopropylacrylamide (97%, Tokyo Kasei Kagyo Co.) was purified by recrystallization in a benzene/*n*-hexane mixture. Silver nitrate ($AgNO_3$, Aldrich) and sodium borohydride ($NaBH_4$, Aldrich) were used as received.

**Synthesis of H40-PNIPAM.** The detailed procedures for the preparation of H40-based macroRAFT agent and H40-PNIPAM star polymers, and the detailed characterization procedures were reported previously.[54,55] The chemical structure of H40-PNIPAM is shown in Figure 1. Two dendritic H40-PNIPAM samples were used in this study and their structural parameters are summarized in Table 1.

**Synthesis of Thiol-Terminated H40-PNIPAM.** Thiolated H40-PNIPAM was prepared by adding excess $NaBH_4$ solution to the aqueous solution of dithioester terminated H40-PNIPAM, which has been deoxygenated by bubbling with high-purity nitrogen for 30 min. The mixture was kept stirring at 5 °C for 48 h under a $N_2$ atmosphere to ensure that the dithioester terminal groups were completely transformed into thiol groups.

**Table 1. Parameters of *H*40-PNIPAM Samples Used in This Work**

| samples | $M_n$[a] (g/mol) | $M_w/M_n$[a] | $M_{w,app}$[b] (g/mol) | DP of PNIAPM[c] | no. of arms[d] |
|---|---|---|---|---|---|
| *H40*-PNIPAM$_{220}$ | $9.20 \times 10^5$ | 1.21 | $1.56 \times 10^6$ | 220 | 50 |
| *H40*-PNIAPM$_{97}$ | $4.75 \times 10^5$ | 1.22 | $6.90 \times 10^5$ | 97 | 52 |

[a] Determined by SEC using DMF + 1.0 g/L BrLi as eluent. [b] Determined in water by static LLS at 15 °C. [c] Degree of polymerization of grafted PNIPAM chains determined by SEC after cleavage via reduction with $KBH_4$. [d] Calculated from $M_{w,app}$ determined by LLS and molecular weight of cleaved PNIPAM arms determined by SEC.

**Conjugation of Gold Nanoparticles onto the Thiol-Terminated Unimolecular Micelles.** In a typical synthesis, calculated amounts of an aqueous solution of thiol-terminated *H*40-PNIPAM at a concentration of $1 \times 10^{-4}$ g/mL were added dropwise into citrate-capped 10 nm gold nanoparticle solution[56] (the ratio of the number of surface thiol groups to gold nanoparticles is ~1.0) under vigorous stirring; this process was conducted under the protection of a $N_2$ atmosphere to minimize the oxidation of thiol groups. After 2 h equilibration at room temperature, the solution mixture was centrifuged at 5000 rpm for 1 h at room temperature and the supernatant solution was discarded. The sediments were then redispersed in water and centrifuged again. This purification cycle was repeated 3 times.

**Size Exclusion Chromatography (SEC).** Molecular weight distributions were determined by SEC using a series of three linear Styragel columns HT3, HT4, HT5 and an oven temperature of 60 °C. Waters 1515 pump and Waters 2414 differential refractive index detector (set at 30 °C) were used. The eluent was DMF + 1 g/L BrLi at a flow rate of 1.0 mL/min. Polystyrene standards are used for calibration.

**Laser Light Scattering (LLS).** A commercial spectrometer (ALV/DLS/SLS-5022F) equipped with a multi-tau digital time correlator (ALV5000) and a cylindrical 22 mW UNIPHASE He−Ne laser ($\lambda_0 = 632$ nm) as the light source was used. In dynamic LLS, the Laplace inversion of each measured intensity−intensity-time correlation function $G^{(2)}(q,t)$ in the self-beating mode can lead to a line-width distribution $G(\Gamma)$. For a pure diffusive relaxation, $\Gamma$ is related to the translational diffusion coefficient $D$ by $(\Gamma/q^2)_{C\to 0,q\to 0} \to D$, or further to the hydrodynamic radius $R_h$ via the Stokes−Einstein equation, $R_h \equiv (k_B T/6\pi\eta_0)/D$, where $k_B$, $T$, and $\eta_0$ are the Boltzmann constant, the absolute temperature, and the solvent viscosity, respectively.

**Transmission Electron Microscopy (TEM).** TEM analyses were conducted on a Hitachi 800 transmission electron microscope at an acceleration of voltage of 200 kV. The sample for TEM observations was prepared by placing 10 $\mu$L of hybrid unimolecular micelle solutions on copper grids coated with thin films of Formvar and carbon, successively.

**UV/vis Spectroscopy.** UV/vis absorption spectra were recorded with a computer-controlled UNICO UV/vis 2802 PCS spectrophotometer.

## Results and Discussion

Au nanoparticles with an average diameter of ~10 nm were prepared according to previously reported procedures.[57,58] Au nanoparticles were then covalently attached

(50) Ornatska, M.; Peleshanko, S.; Rybak, B.; Holzmueller, J.; Tsukruk, V. V. *Adv. Mater.* **2004**, *16*, 2206-+.
(51) Ornatska, M.; Peleshanko, S.; Genson, K. L.; Rybak, B.; Bergman, K. N.; Tsukruk, V. V. *J. Am. Chem. Soc.* **2004**, *126*, 9675−9684.
(52) Ornatska, M.; Bergman, K. N.; Rybak, B.; Peleshanko, E.; Tsukruk, V. V. *Angew. Chem., Int. Ed.* **2004**, *43*, 5246−5249.
(53) Xu, J.; Luo, S.; Shi, W.; Liu, S. *Langmuir* **2006**, *22*, 989−997.
(54) Luo, S. Z.; Xu, J.; Zhu, Z. Y.; Wu, C.; Liu, S. Y. *J. Phys. Chem. B* **2006**, *110*, 9132−9139.
(55) Xu, J.; Luo, S. Z.; Shi, W. F.; Liu, S. Y. *Langmuir* **2006**, *22*, 989−997.
(56) Grabar, K. C.; Freeman, R. G.; Hommer, M. B.; Natan, M. J. *Anal. Chem.* **1995**, *67*, 735.

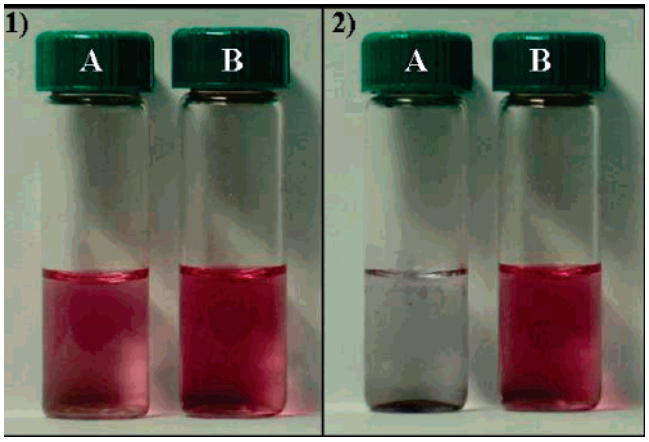


**Figure 2.** Ten nanometer Au nanoparticle solution (A) and hybrid unimolecular micelles of *H40*-PNIPAM$_{220}$ surface-attached with Au nanoparticles. (B) The NaCl concentrations in (1) and (2) ae 0 and 0.5 M, respectively.

to the thiolated surface of unimolecular micelles. The core of the unimolecular micelle template consisted of fractionated Boltorn H40, a fourth generation hyperbranched polyester, and the shell consists of densely grafted poly(*N*-isopropylacrylamide) (PNIPAM) chains.[54,55] Controlling the spatial distance between surface-decorated Au nanoparticles is achieved by taking advantage of the phase transition of the PNIPAM shell at its lower critical solution temperature (LCST) of ~32 °C. At room temperature, the PNIPAM shell is water-swollen, whereas at temperatures above the LCST, the PNIPAM shell collapses.[54] Our previous studies of the unimolecular micelles of H40-PNIPAM demonstrated that the thermal phase transition of the PNIPAM shell is completely reversible.[54,55]

PNIPAM chains were grafted onto the surface of hydrophobic H40 core via reversible addition−fragmentation chain transfer (RAFT) technique using the H40-based macroRAFT agent.[54,55] Two H40-PNIPAM star-block copolymers were synthesized with the average degree of polymerization (DP) of grafted PNIPAM chains being 220 and 97, and they were denoted H40-PNIPAM$_{220}$ and H40-PNIPAM$_{97}$, respectively (Table 1). In aqueous solution, H40-PNIPAM star polymer molecularly dissolves, forming unimolecular micelles with H40 as the core and the grafted PNIPAM chains as the corona. The dithioester groups attached at the surface of unimolecular micelles were then conveniently transformed to thiol groups upon addition of excess sodium borohydride ($NaBH_4$).[59−61] Subsequent addition of calculated amount of thiol-terminated H40-PNIPAM into the citrate-capped gold nanoparticle solutions (at a ratio of [gold nanoparticles]/[thiol] ≈ 1.0) under a $N_2$ atmosphere leads to the facile preparation of hybrid unimolecular micelles surface attached with gold nanoparticles.

(57) Brown, K. R.; Walter, D. G.; Natan, M. J. *Chem. Mater.* **2000**, *12*, 306−313.
(58) Grabar, K. C.; Freeman, R. G.; Hommer, M. B.; Natan, M. J. *Anal. Chem.* **1995**, *67*, 735−743.
(59) Lowe, A. B.; Sumerlin, B. S.; Donovan, M. S.; McCormick, C. L. *J. Am. Chem. Soc.* **2002**, *124*, 11562−11563.
(60) Zhu, M. Q.; Wang, L. Q.; Exarhos, G. J.; Li, A. D. Q. *J. Am. Chem. Soc.* **2004**, *126*, 2656−2657.
(61) Shan, J.; Chen, J.; Nuopponen, M.; Tenhu, H. *Langmuir* **2004**, *20*, 4671−4676.

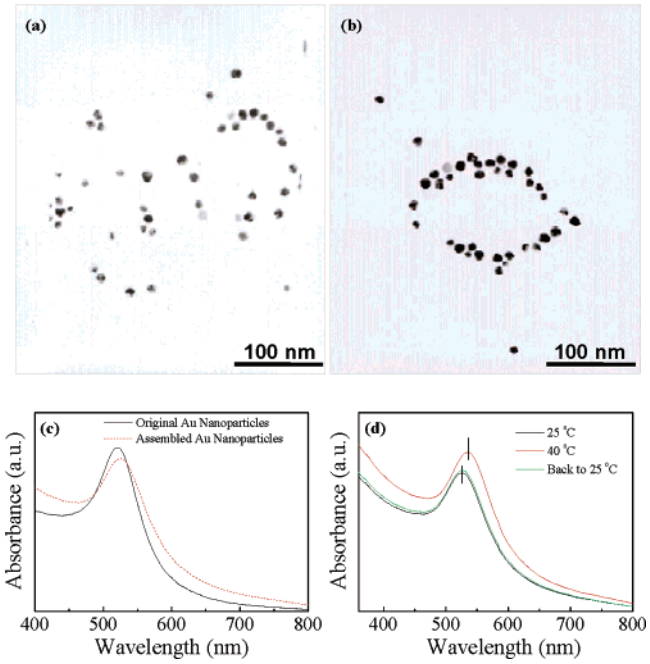


**Figure 3.** (a, b) Typical TEM images of the satellite-like nanostructures assembled from surface thiolated unimolecular micelles of *H40*-PNIPAM$_{220}$ and Au nanoparticles. (c) UV/vis absorption spectra of the original Au nanoparticles and hybrid unimolecular micelles surface-attached with Au nanoparticles at 25 °C. (d) UV/vis absorption spectra of hybrid unimolecular micelles of *H40*-PNIPAM$_{220}$ recorded at different temperatures.

The unimolecular micelles of H40-PNIPAM$_{220}$ have an average hydrodynamic diameter, $<D_h>$, of ~140 nm at 25 °C, as determined by dynamic LLS. The number of grafted PNIPAM chains per H40 core was determined to be ~50.[54] The surface area occupied per terminal thiol group was thus calculated to be ~1200 nm$^2$, i.e., the average distance between two neighboring surface thiol groups was ~35 nm. Compared to the size of citrate-capped gold nanoparticles (10 nm), it is reasonable to speculate that the surface-attached gold nanoparticles are well-separated and each gold nanoparticle will most probably conjugate with only one thiol group.[19] At least this type of conjugation should be the major product.

After conjugating the gold nanoparticles onto the surface of thiolated unimolecular micelles of H40-PNIPAM$_{220}$, there is no visual change of the appearance as compared to that of the original gold nanoparticles. Because the original nanoparticles were citrate-stabilized, they were quite sensitive to the addition of salt (e.g., NaCl) and will aggregate immediately and irreversibly.[2,62] Further increasing the salt concentration will eventually precipitate out the gold nanoparticles. The comparison of the stability between the citrate-capped gold nanoparticles and the obtained hybrid unimolecular micelles upon addition of NaCl was shown in Figure 2. In the presence of 0.5 M NaCl, the original gold nanoparticles completely precipitated out of the solution and we observed the quick formation of black sediments. However, the unimolecular micelle template-stabilized gold nanoparticle solution is extremely stable, showing no apparent changes as compared to that in the absence of salt (Figure 2). This strongly suggested that gold nanoparticles

(62) Wang, G.; Sun, W. *J. Phys. Chem. B* **2006**, *110*, 20901−20905.

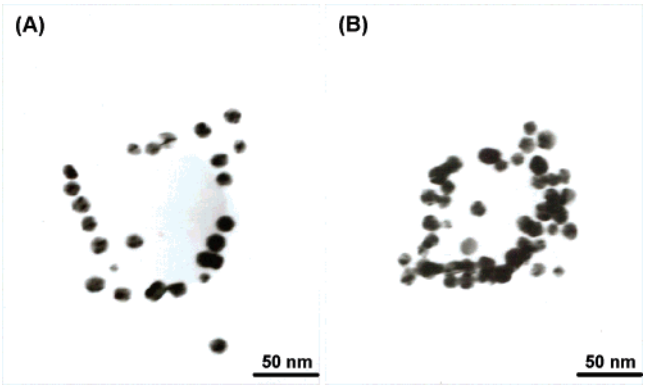


**Figure 4.** TEM images of the ringlike nanostructures assembled from thiolated *H40*-PNIPAM$_{220}$ unimolecular micelles and Au nanoparticles.

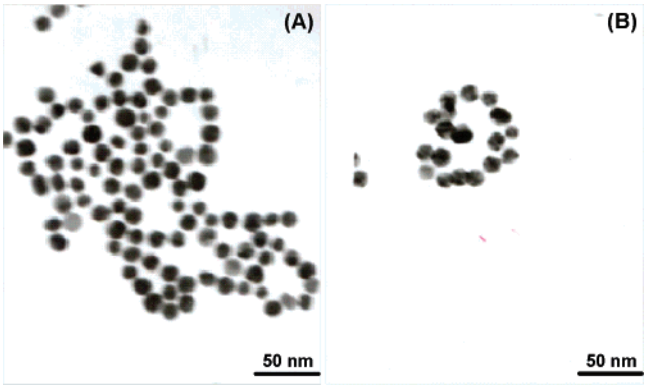


**Figure 5.** TEM images of the ringlike nanostructures assembled from thiolated *H40*-PNIPAM$_{97}$ unimolecular micelles and Au nanoparticles.

have been covalently attached to the surface of unimolecular micelles through covalent Au−thiol interactions. Hybrid unimolecular micelles surface attached with gold nanoparticles should have formed as shown in Scheme 1.

Images a and b of Figure 3 show the TEM images of the assembled satellite-like nanostructures of gold nanoparticles after depositing the hybrid unimolecular micelle solution onto a carbon-coated copper grid at 25 °C. It can be seen that gold nanoparticles with an average diameter of 10 nm are localized into a ringlike array on the surface of a copper grid. More TEM images at higher magnifications are shown in Figure 4. On average, there are ∼25−40 gold nanoparticles conjugated per unimolecular micelle of H40-PNIPAM$_{220}$, suggesting a relatively high conjugation efficiency considering that there are ∼50 thiol groups at the surface of unimolecular micelles. The size of the almost-circular gold nanoparticle arrays is generally comparable to the size of the unimolecular micelles (140 nm) as determined by dynamic LLS. Recently, thiolated polymer chains have been extensively employed as templates for the assembly of gold nanoparticles.[20,21,63] Huo et al.[18,19] reported that the covalent conjugation of monofunctionalized gold nanoparticles to polymer chains is a facile and effective approach to fabricate nanoparticle assemblies.

When H40-PNIPAM$_{97}$ was employed as a template to assemble gold nanoparticles, smaller ringlike nanostructures were observed by TEM (Figure 5). The number of gold nanoparticles conjugated per unimolecular micelles of H40-PNIPAM$_{97}$ was determined to be ∼20. Thus, the average number of gold nanoparticles conjugated can be controlled by the size of unimolecular micelles. All of these strongly suggested that the covalently attached gold nanoparticles serve as a good indicator for directly visualizing the dimensions of unimolecular micelles.

Figure 3c shows the corresponding UV/vis absorption spectra of the original gold nanoparticles and hybrid unimolecular micelles. The absorption spectrum of the original gold nanoparticle solution exhibited a maximum at 519 nm, which is characteristic of gold nanoparticles with a diameter of ∼10 nm.[57,58] After gold nanoparticles were conjugated to the surface of thiolated unimolecular micelles, the surface plasmon band showed a small but discernible shift to 524 nm. This indicated that the conjugation of gold nanoparticles onto the unimolecular micelle surface has increased the local concentration of gold nanoparticles at the micelle surface and decreased the average spatial distance between gold nanoparticles compared to that in the original gold nanoparticle solutions.[2] It should be noted that the UV/vis absorption spectrum does not show any noticeable aggregation between the conjugated gold nanoparticles,[62] which is also consistent with the TEM results (Images a and b of Figure 3).

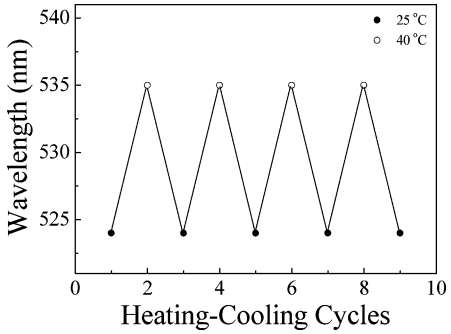


**Figure 6.** Maximum wavelength of the surface plasmon peak as a function of heating−cooling cycles for hybrid unimolecular micelles of *H40*-PNIPAM$_{220}$ between 25 and 40 °C.

Upon increasing the solution temperature from 25 to 40 °C, dynamic LLS studies revealed that the size of the unimolecular micelles of H40-PNIPAM$_{220}$ shrinked gradually from 140 to ∼100 nm.[54,55] Because of the covalent binding of gold nanoparticles to the thiol groups at the surface of unimolecular micelles, the shrinkage of PNIPAM corona will concomitantly decrease the average distance between gold nanoparticles (Scheme 1). The calculated average spatial distance between neighboring gold nanoparticles will thus decrease from 35 to ∼20 nm. This distance is about twice that of the diameter of gold nanoparticles, suggesting that surface attached neighboring gold nanoparticles will come in contact with each other at 40 °C. We indeed observed a further red-shift of the maximum of surface plasmon band from 524 to 535 nm when the temperature increased from 25 to 40 °C (Figure 3d).[2] Previous results indicate that the change of refractive index can induce the red-shift of surface plasmon peak only up to 5 nm even though the external temperature is increased to 60 °C.[64] So the dramatic red-shift at increasing temperatures for hybrid unimolecular micelles should be mainly due to the decrease of relative

(63) Zin, M. T.; Yip, H. L.; Wong, N. Y.; Ma, H.; Jen, A. K. Y. *Langmuir* **2006**, *22*, 6346−6351.

distances between gold nanoparticles and the enhanced interparticle coupling, which is driven by the shrinkage of PNIPAM brush of unimolecular micelles (Scheme 1).

As the temperature decreases from 40 to 25 °C, the surface plasmon band shifted back to the original position at 524 nm (Figure 3d). We further found that this process can be reliably repeated (Figure 6), even after more than 20 heating−cooling cycles. No apparent macroscopic phase separation can be observed. This should be due to the structural stability of unimolecular micelles, which serves as an excellent scaffold to the covalently conjugated gold nanoparticles. Thus, we can conveniently tune the interparticle distance by changing the external temperatures.

## Conclusion

In conclusion, we reported a facile approach to the formation of highly stable satellite-like nanostructures of gold nanoparticle arrays. This technique utilizes thiol-functionalized thermosensitive unimolecular micelles as templates for the covalent attachment of gold nanoparticles at the surface. The assembled satellite-like nanostructures exhibit thermosensitive properties with complete reversibility. The spatial distance between neighboring gold nanoparticles can be finely tuned with temperature. This novel type of thermosensitive hybrid nanostructures with high stability may have potential use for stimuli-responsive applications. It should also be possible to extend this approach to fabricate novel functional nanomaterials with sophisticated structures and tunable multifunctionalities.

**Acknowledgment.** This work was financially supported by an Outstanding Youth Fund (50425310) and research grants (20534020, 20674079) from the National Natural Scientific Foundation of China (NNSFC), the "Bai Ren" Project of the Chinese Academy of Sciences, and the Program for Changjiang Scholars and Innovative Research Team in University (PCSIRT).

CM070088G

(64) Kuang, M.; Wang, D. Y.; Mohwald, H. *Adv. Funct. Mater.* **2005**, *15*, 1611.